ZandiPaper.docx

WORD COUNT	7705	TIME SUBMITTED	29-DEC-2025 05:29PM
		PAPER ID	119692352

Decision-Inspired Ensemble Framework for Reliable Urban Land Surface Temperature Prediction: Insights from Tehran, Iran

~~Decision-Inspired Ensemble Learning for Urban Land Surface Temperature Prediction (A Case Study of Tehran-Iran)~~

Formatted: Shadow

Abstract

Climate change and increasing land surface temperature (LST) have become major environmental concerns in large metropolitan areas, particularly in arid and semi-arid regions. Reliable prediction of LST is essential for urban climate assessment, mitigation of the urban heat island effect, and informed urban planning. This study develops an interpretable machine learning–based framework for predicting LST across Tehran, Iran, using multiple base models and novel ensemble strategies. Five widely used machine learning algorithms—Artificial Neural Networks (ANN), Random Forest (RF), Support Vector Machine (SVM), Classification and Regression Tree (CART), and Generalized Linear Model (GLM)—were first trained using identical datasets to capture the spatial variability of LST and its driving factors. Model performances were evaluated separately across different urban zones of Tehran using statistical accuracy metrics. These performance scores were then used as inputs to four newly designed ensemble models inspired by collective human decision-making systems, including presidential voting, parliamentary voting, hierarchical governance, and ancient senate-based consensus mechanisms. The proposed ensemble frameworks consistently improved prediction accuracy compared to individual models, while also increasing robustness across heterogeneous urban landscapes. The results demonstrate that decision-inspired ensemble learning can enhance both accuracy and confidence in LST predictions. The proposed approach offers a transparent and transferable tool for urban climate analysis and can support evidence-based decision-making for heat mitigation strategies in large cities.

Keywords: Land Surface Temperature, Ensemble learning, Machine learning, Urban climate, Tehran

~~*Abstract*~~

1. Introduction

Land surface temperature (LST) is a key indicator of urban thermal conditions and plays a central role in assessing the impacts of climate change and urbanization on metropolitan environments. In rapidly expanding cities, increased impervious surfaces, reduced vegetation cover, and intensified anthropogenic activities significantly alter surface energy balances, leading to elevated LST and the urban heat island (UHI) effect (Oke, 1982). Recent studies have shown that global urban expansion has accelerated considerably, intensifying thermal stress in large cities and increasing exposure to heat-related risks for urban populations.

Elevated LST has been associated with a range of negative environmental and socio-economic consequences, including increased energy demand for building cooling, degradation of air quality, heightened risks of heat-related illnesses, and reduced thermal comfort and quality of life. These impacts are particularly pronounced in megacities located in arid and semi-arid regions, where background climatic conditions already impose thermal stress.

Accurate prediction of LST in urban areas remains challenging due to the spatial heterogeneity of land use, complex interactions between natural and anthropogenic factors, and non-linear relationships among influencing variables. Conventional physics-based and energy balance models often require extensive input data and high computational costs, which may limit their applicability at fine spatial

scales or for large urban regions. Consequently, data-driven approaches, particularly machine learning (ML) methods, have increasingly been adopted to model LST dynamics.

Machine learning algorithms such as Random Forest, Support Vector Machine, and Artificial Neural Networks have demonstrated strong capability in capturing complex non-linear relationships between LST and its controlling factors. However, the predictive performance of these algorithms can vary substantially depending on data characteristics, spatial context, and parameter tuning. Moreover, reliance on a single algorithm may introduce uncertainty and reduce robustness, particularly in heterogeneous urban environments.

Tehran, the capital of Iran, is a densely populated megacity characterized by diverse land use patterns, complex topography, and a semi-arid climate. Numerous studies have reported an increasing temperature trend in Tehran over recent decades, accompanied by intensified UHI effects. Despite growing interest in applying ML techniques for LST prediction in Tehran, several challenges remain, including data heterogeneity, algorithm selection, parameter optimization, and model interpretability.

To address these challenges, this study proposes a comparative and ensemble-based ML framework for LST prediction in Tehran. Multiple base learners are first evaluated independently to identify their strengths and weaknesses across different urban zones. Building on these results, four novel ensemble models inspired by collective human decision-making systems are introduced to integrate model outputs in a structured and transparent manner. Unlike conventional ensemble methods that rely solely on statistical averaging, the proposed approach incorporates decision-weighting concepts derived from governance and voting systems.

The objectives of this study are to:

(1) evaluate the performance of commonly used ML algorithms for LST prediction in Tehran;

(2) investigate the contribution of key explanatory variables to LST variability; and

(3) assess whether decision-inspired ensemble models can outperform individual ML models and enhance prediction reliability.

The proposed framework aims to provide a robust and interpretable tool for urban climate assessment and offers practical insights for urban planners and policymakers seeking to mitigate heat-related risks in large cities.

2. Review of Literature

In recent years, machine learning (ML) techniques have been increasingly employed for land surface temperature (LST) prediction due to their ability to capture complex and non-linear relationships between thermal patterns and environmental variables. Advances in artificial intelligence have expanded the applicability of ML models across a wide range of spatial and temporal scales, enabling more flexible and accurate modelling compared to conventional approaches (Fleming et al., 2021; Gevaert, 2022; Gunning et al., 2019; McGovern et al., 2019). As global temperature rise has become a widely acknowledged environmental challenge, research efforts have increasingly focused on improving the accuracy and reliability of LST estimation methods.

Early comparative studies highlighted the advantages of ML-based approaches. For example, Weng et al. (2004) evaluated several ML models in Chinese cities and demonstrated that data-driven methods outperform traditional statistical approaches in urban LST analysis. Subsequent research has not only improved prediction accuracy but also examined the broader

implications of rising surface temperatures and potential mitigation strategies. Santamouris (2001), for instance, investigated the climatic and energy impacts of urban environments, emphasizing the role of urban form and design in mitigating urban heat island (UHI) effects. Similarly, Kovats and Hajat (2008) established a clear link between increasing temperatures and the incidence of heat-related illnesses, highlighting the public health implications of urban warming.

More recent studies have integrated remote sensing data with ML techniques to explore the drivers of LST variability. Zhang et al. (2017) analyzed land use changes and their influence on LST in Beijing, demonstrating that urban expansion and surface modification significantly affect thermal patterns. Zubair Irshad et al. (2024) examined land use and land cover (LU/LC) changes in several regions of Pakistan and reported substantial LST increases between 2000 and 2020, with the highest values observed in densely built urban areas and the lowest in vegetated or water-covered regions.

In Iran, a growing body of literature has addressed temperature variability and urban warming. Aliakbari Bidokhti et al. (2016) analyzed long-term temperature and precipitation trends in Tehran, confirming an overall warming trend and emphasizing the need for reliable modelling tools. Roshan et al. (2024) investigated UHI intensity during heatwave events in Tehran and showed that thermal patterns vary across different climatic conditions and are strongly influenced by anthropogenic structures and industrial activities. Likewise, Kiavarz et al. (2022) employed satellite imagery to analyze and predict temperature changes in Tehran, concluding that the observed warming trend is likely to continue in the future.

Alongside advances in individual ML models, ensemble learning approaches have gained attention as an effective means of improving predictive performance. Ensemble models combine multiple learners to reduce uncertainty, compensate for individual model weaknesses, and enhance result robustness. Numerous studies have demonstrated the effectiveness of ensemble techniques in environmental applications, reporting improvements in prediction accuracy and interpretability (Ashrafzadeh et al., 2023). In Iran, while ensemble models have been applied to several environmental and ecological problems, their use in LST prediction—particularly at the city scale in Tehran—remains limited.

A notable example of ensemble modelling in Iran is the work by Ashrafzadeh et al. (2023), who investigated the spatial distribution of brown bears in the Zagros Mountains using multiple ensemble approaches. Their results showed that combining several models yields more reliable predictions than relying on a single algorithm. Similar conclusions have been reported in other environmental studies, where ensemble learning reduced bias and uncertainty and increased confidence in model outputs by requiring agreement among multiple predictors (Di Napoli et al., 2020).

Previous efforts have also contributed methodological advancements to this field. Thuiller et al. (2009) developed an ensemble-based modelling framework for ecological applications through the Biomod2 platform in R, demonstrating its effectiveness in handling environmental complexity. Despite these advancements, critical urban challenges such as surface warming in densely populated Iranian cities have received comparatively less attention within an ensemble-learning framework. Applying advanced ensemble methods to LST prediction can therefore improve understanding of urban thermal dynamics and provide a stronger scientific basis for mitigation and planning strategies.

3. Methodology

3.1. Study Area

Tehran, the capital of Iran, is the country's largest and most populous city, facing numerous environmental and climate change challenges. Geographically located on the southern slopes of the Alborz Mountain range within a closed basin, Tehran experiences temperature inversions and increased air pollution during colder seasons. These factors, combined with rapid urbanization, extensive construction, and diminishing green spaces, have contributed to rising land surface temperatures (LST) and the formation of urban heat islands (UHI). Tehran comprises 22 districts and 374 neighborhoods, as illustrated in Figure 1.

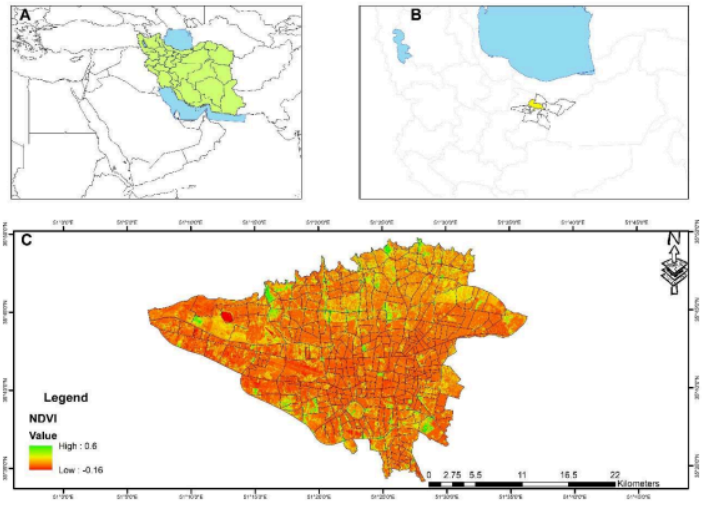

Figure 1. Location of the study area

3.2. Materials and Methods

This study introduces four novel ensemble models inspired by human collective systems, including the U.S. presidential election, the U.S. Congress, monarchical governance, and the ancient Senate system, to predict LST in the Tehran metropolitan area. LST and its influencing factors were initially analysed using machine learning algorithms, specifically ANN, RF, SVM, Classification and Regression Tree (CART), and Generalized Linear Model (GLM). The analysis for each model involved five stages: preparation of initial data, selection of parameters affecting LST, preparation of training and testing datasets, execution of machine learning models, and presentation of LST results in a map format.

Subsequently, the outputs of these models were statistically evaluated and processed to determine the accuracy of each model across different regions. These results were then used as input parameters for the ensemble algorithms. The ensemble models, including those inspired by the U.S. presidential

election, U.S. Congress, monarchical governance, ancient Senate system, mean, median, and weighted mean approaches, were applied, followed by validation. Finally, the significance of various parameters was estimated and presented using five different algorithms and seven ensemble models.

3.2.1. Preparation of Geospatial Database

This study utilized 20 Landsat 8 satellite images from 2020 to determine LST and the Normalized Difference Vegetation Index (NDVI), as detailed in Table 1.

Table 1. Landsat 8 images specifications

	Satellite	Sensor	Date	Spatial resolution
1	Landsat 8	OLI	14-Jan-20	Multispectral: 30 m Thermal band: 100m
2			30-Jan-20	
3			15-Feb-20	
4			2-Mar-20	
5			18-Mar-20	
6			3-Apr-20	
7			19-Apr-20	
8			5-May-20	
9			21-May-20	
10			6-Jun-20	
11			22-Jun-20	
12			8-Jul-20	
13			24-Jul-20	
14			9-Aug-20	
15			25-Aug-20	
16			10-Sep-20	
17			26-Sep-20	
18			12-Oct-20	
19			28-Oct-20	
20			15-Dec-20	

Image processing was conducted using Google Earth Engine. The resolution of bands 1 to 9 is 30 meters, providing sufficient accuracy, while the thermal bands have a resolution of 100 meters, suitable for analysis temperature variations across Tehran. Band 10 was used to extract surface temperature data with a wavelength range of 10.6 to 11.9 micrometres and a 100-meter resolution. Atmospheric corrections were performed using the FLAASH method prior to processing in Google Earth Engine. Geometric corrections were applied, and the Maximum Likelihood Classification (MLC) method, a widely used approach, was employed.

Urban morphology data, including building height (BH), building density (BD), and sky view factor (SVF), were derived from building block height information. Urban road length and area (Integ_Rn), two independent parameters, were obtained from Tehran's 2014 development plan and used to calculate Integration Rn. Additionally, urban green spaces and their patterns, represented by NDVI, Mean Patch Index (MPI), and Mean Patch Fractal Dimension (MPFD), were included as influential parameters, as outlined in Table 2.

Table 2. the urban form indicators selected in this study

Category	Index	Description	Unit	range	Equation
Urban morphology	Building height(BH)	Expresses height of building	m	$0 < BH$	-
	Building density(BD)	Shows by the proportion of building square footage in a block, neighborhood or district. BD defines crowded or built-up a neighborhood, land intensity and worth of land or building	None	$0 \leq BD$	$\frac{Build\ up\ area}{land\ area}$
	Sky view factor(SVF)	Addresses to the ratio of the radiation received (or emitted) by a planar surface to the radiation emitted (or received) by the entire hemispheric environment. SVF is more appropriate tools for describing urban geometry	Degree	$0 < SVF \leq 1$	$2\pi - \sum_{d}^{ND} S_{Hd}$ Where ND is the number of sky hemisphere sectors, d is a given azimuthal ray direction and SHd is the surface of sky hemisphere hidden by obstacles in the azimuthal direction d.
Urban road	Road length (RL)	measures the sum of urban road length in the neighborhood.	m	$0 < RL$	$\sum_{i=1}^{n} L_i$ L_i is length of the road in urban neighborhood
	Road area (RA)	Presents total area of the urban roads in the neighborhood scale. Increasing RA has positive effect on LST	m^2	$0 < RA$	$\sum_{i=1}^{n} L_i W_i$ Where Li is length of the road and Wi is width of the road.
Spatial configuration	Integration-Rn(Integ_Rn)	Describes the average depth of a space to all other space. A value which is used to measure of spatial configuration. Rn be used to represent integration patterns in the large scale; define small, close areas with geometric center	None	$0 < Int - Rn$	$\frac{1}{RRA_{Rn}}$ RRA is a normalized measure since it is calculated as RA normalized though the D-Value. Integration-Rn is inverse of RRA(Hillier and Hanson 1984).
Urban vegetation and spatial patterns	NDVI	Is an useful index to quantify vegetation greenness, it's density, changes and health.	None	$-1 \leq NDVI \leq +1$	NDVI is evaluated as a ratio between the red (R) and near infrared (NIR) values in traditional fashion: $R_{NIR} - R_{RED}/R_{NIR} + R_{RED}$

	MPI	Measures the degree of isolation and fragmentation of urban vegetation.	None	$0 < MPI$	$\sum_{i=1}^{n} \frac{a_i}{h_{ij}^2}$ In this equation, n, is total number of patches, ai, is patch area, and *hij*, is distance from the patch *i* to the patch *j*.
	MPFD	This metric quantifies the complexity of the shape, with values ranging from 1 to 2. A value of 1 corresponds to patches with simple perimeters, such as squares, while a value approaching 2 indicates increasingly complex shapes.	None	$1 \leq MPFD \leq 2$	$\frac{\sum_{j=1}^{m}(\frac{2lnp_{ij}}{lna_{ij}})}{n_i}$ where *Pij* is the patch perimeter of type *ij*, in units of m; *aij* is the patch area of type *ij*; and N is the number of patches of a certain type.

3.2.2. Distribution of Independent Parameters

The independent parameters exhibit varying spatial distributions, as shown in Figure 2. BH, BD, and Integ_Rn vary significantly across Tehran, with notable changes from the city centre to its outskirts. Conversely, road area, NDVI, and MPI exhibit higher values in the city centre.

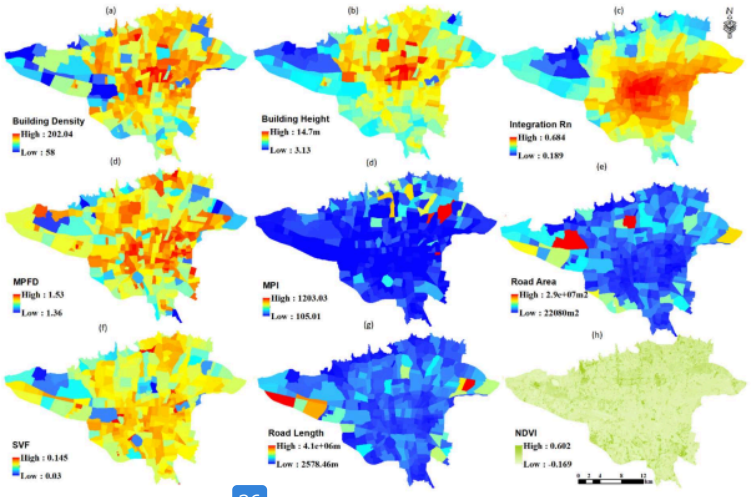

Figure 2- Spatial distribution of the selected variables

3.2.3. Structure of Ensemble Models

The following ensemble models were developed and applied:

3.2.3.1. Mean Method

In this method, the numerical mean of the outputs from all models was calculated and presented as a map. The value of each cell represents the average of the five models. The accuracy of this method generally depends on the average accuracy of all models.

3.2.3.2. Weighted Mean Method (WMean)

This ensemble method calculates a weighted mean based on the accuracy of each model (R-squared). The outputs of the five models were mapped, with higher-accuracy models exerting greater influence on the final ensemble result. This approach enhances the impact of more accurate models on the ensemble outcome.

3.2.3.3. Median Method

This method selected the model output with the least deviation from the weighted mean as the ensemble result. The weighted mean was first calculated, followed by the deviation of each model from this mean. The model's output with the smallest deviation was presented as the ensemble result.

3.2.3.4. Genius King Method

Inspired by the concept of a wise monarch, this method leverages the strengths of each model in regions where it performs most accurately. By considering the performance of each model across different areas of the city, the method selects the output of the model with the lowest error (RMSE) for each region. In cases where identifying a superior model is not feasible, the method defaults to the mean of all model outputs, as depicted in Figure 3.

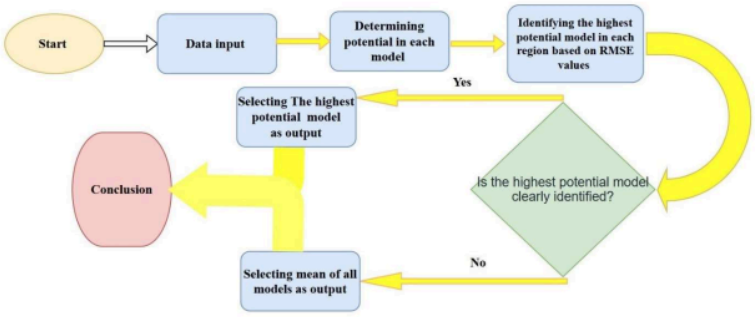

Figure 3. Flowchart for the Genius King Ensemble Method

3.2.3.5. Ancient Senate Method

In this method, inspired by the ancient Senate system, a polling process is conducted on a specific issue (hazard). Like human collectives, the group of models with the majority vote is declared the winner, and a decision is made on the issue. This study defined a temperature exceeding 20°C as a hazard. A vote was then taken, and the majority (at least three votes in favour or against) was identified as the winner. Finally, the mean of the winning models was calculated. Given that five models were used in this study, the criterion for winning was at least three aligned votes. Thus, the result for each cell could be the mean of three, four, or five models with aligned votes (either in favour or against), as shown in Figure 4.

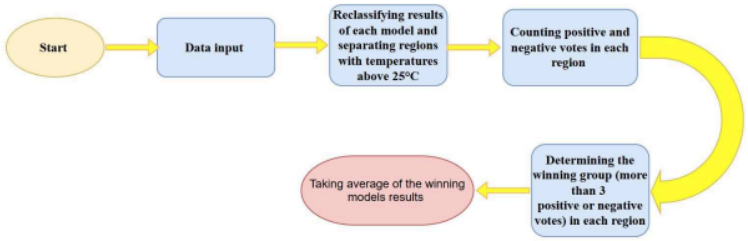

Figure 4. Flowchart of the Ancient Senate Method

3.2.3.6. The U.S. Congress Method

This method is modelled after the decision-making process in the U.S. Congress. In the U.S. Congress, significant decisions are delegated to specialized committees. If a specialized committee is not formed or does not exist for a given issue, a general vote is conducted, with each model's vote carrying equal weight. In this study, a specialized committee was first formed for each domain, decisions were made within the committee, and the mean of the committee members' outputs was presented as the ensemble result. In regions where identifying superior models and forming an ensemble was not feasible, the mean of all models was used as the result, as shown in Figure 5.

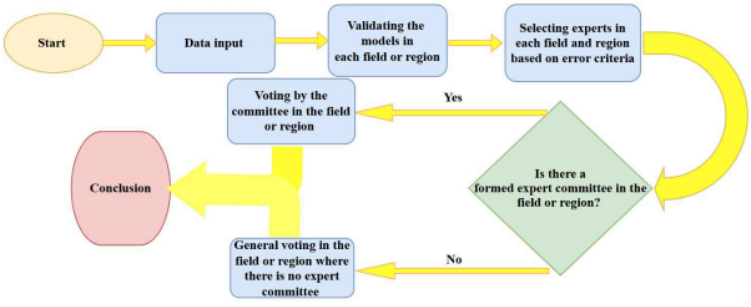

Figure 5: Flowchart of the U.S. Congress Method

3.2.3.7. The U.S. Presidential Election Method

This method is inspired by the U.S. presidential election system, where electoral votes are assigned to each model based on accuracy. The number of electoral votes for each model is determined as a function of its ability to detect a hazard or non-hazard, using the True Positive Rate (TPR) and True Negative Rate (TNR) as weighting factors. The total number of electoral votes was set to 538. A vote was then conducted: if the positive votes (indicating a hazard) exceeded 269, the weighted mean of the models with positive votes was calculated using TPR as the weighting factor. Conversely, if the negative votes (indicating no hazard) prevailed (positive votes < 270), the weighted mean of the models with negative votes was calculated using TNR as the weighting factor, as shown in Figure 6. This method enhances talent identification by considering two model capabilities: the ability to detect and negate a hazard. TPR is the weighting factor in hazard regions, while TNR is used in the non-hazard regions.

- Equation 1: TPR = TP / (TP + FN)
- Equation 2: TNR = TN / (TN + FP)

Where TP represents true positives, FN represents false negatives, FP represents false positives, and TN represents true negatives.

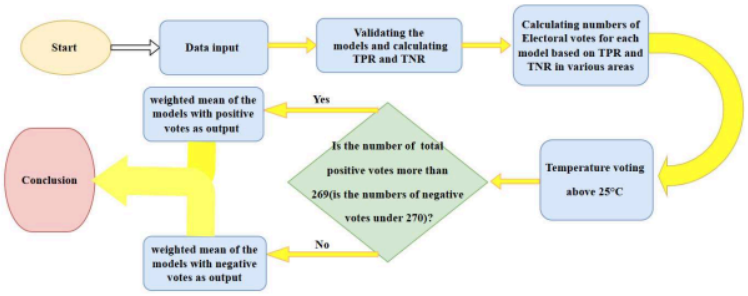

Figure 6: Flowchart of the U.S. Presidential Election Method

3.3. Evaluation and Comparison of Models

This study's dataset was first divided into two subsets: training and testing. After training the models using the training data (70% of the dataset), the accuracy of each model was evaluated by predicting and comparing the testing data (30% of the dataset) to assess their performance in predicting Land Surface Temperature (LST). The performance of five machine learning models and seven ensemble models was compared using statistical metrics, including Mean Absolute Error (MAE), Mean Squared Error (MSE), Root Mean Square Error (RMSE), and R-squared (R^2). Additionally, to evaluate each model's ability to predict temperatures above 20°C as a hazard accurately, the True Positive Rate (TPR) was calculated for the five models. Similarly, the True Negative Rate (TNR) was used to assess the models' ability to predict regions with temperatures below 20°C.

3.4. Analysis of Parameter Importance in Prediction (VIP)

The study also analysed the factors influencing LST in Tehran. To this end, the importance of each parameter (VIP) was determined by calculating the change in the model's error (RMSE) when that parameter was excluded. Specifically, the increase in the model's error upon removing a parameter reflects its importance, as the model's accuracy is affected proportionally to the significance of the excluded parameter.

4. Results

4.1. Analysis of LST Using the RF Model

In this study, the RF model was employed to analyse LST. The results were presented as three temperature classes in map format (Figure 7 and Table 3). According to the findings, 64% of the study area has temperatures below 20°C, 35% fall between 20°C and 25°C, and 1% exceed 25°C.

4.2. Analysis of LST Using the ANN Model

The ANN model was also successfully applied in this study. The results were similarly presented as three temperature classes in map format (Figure 7 and Table 3). According to this model, 65% of the area has temperatures below 20°C, 30% ranges between 20°C and 25°C, and 5% exceeds 25°C. Compared to the RF model, the ANN model adopts a more conservative approach, identifying larger areas at risk of increased LST.

4.3. Analysis of LST Using the SVM Model

The SVM model was another method utilized in this study. The results were presented as three temperature classes in map format (Figure 7 and Table 3). According to the findings, 68% of the area has temperatures below 20°C, 31% ranges between 20°C and 25°C, and 1% exceeds 25°C. Compared to the RF model, the SVM model identifies smaller areas at risk of increased LST.

4.4. Analysis of LST Using CART

The results of LST prediction using the CART model were also presented in three temperature classes (Figure 7 and Table 3). According to the results, 65% of the area has temperatures below 20°C, and approximately 35% falls between 20°C and 25°C. Notably, this model did not predict any areas with temperatures exceeding 25°C, indicating its lack of accuracy in identifying regions with temperatures above 25°C.

4.5. Analysis of LST Using the GLM

The GLM was also used to analyse LST in this study. The results were presented as three temperature classes in map format (Figure 7 and Table 3). According to the findings, 65% of the area has temperatures below 20°C, 34% ranges between 20°C and 25°C, and 1% exceeds 25°C. Compared to the other models, the GLM model demonstrates a higher correlation in identifying areas with temperatures above 25°C.

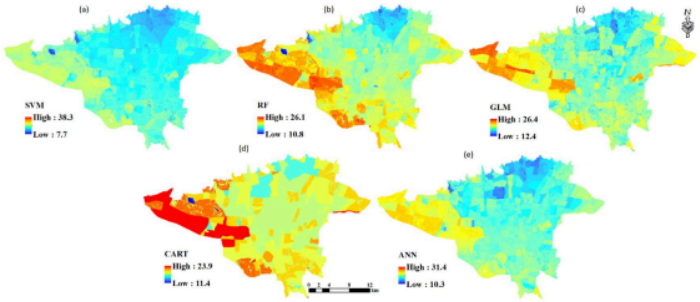

Predicted LST using different Algorithms. Fig. 7-

Model	ANN	CART	SVM	GLM	RF
<20 C	65	65	68	65	64
20-25 C	30	35	31	34	35
>25C C	5	0	1	1	1

Table 3: Distribution of Predicted LST Using Different Models

4.6. Validation Assessment

Various statistical methods were employed to validate the accuracy of the models in this study. Five machine learning models, ANN, RF, CART, SVM, and GLM, were validated using MAE, MSE, RMSE, and R-squared (R^2) metrics. These metrics reflect the models' ability to predict LST. The MAE values for RF, SVM, ANN, CART, and GLM were 1.11, 1.28, 1.62, 1.68, and 1.77, respectively. The MSE values for these models were 2.33, 3.13, 4.54, 4.76, and 5.4, respectively. The RMSE values were also 1.06, 1.13, 1.27, 1.30, and 1.33 for RF, SVM, ANN, CART, and GLM, respectively. These results indicate that all five models are sufficiently accurate, with the RF model outperforming the others in predicting LST for this case study. The R^2 values for RF, SVM, ANN, CART, and GLM were 0.76, 0.68, 0.55, 0.50, and 0.44, respectively, further confirming the sufficient accuracy of all models and the superiority of the RF model in LST prediction (Table 4).

The sensitivity (TPR) of the ANN, RF, CART, SVM, and GLM models was 0.744, 0.825, 0.729, 0.819, and 0.719, respectively, while the specificity (FPR) was 0.161, 0.100, 0.176, 0.150, and 0.178, respectively. The TNR values for these models were 0.839, 0.900, 0.824, 0.850, and 0.822, respectively. These metrics demonstrate the models' sufficient accuracy in predicting temperatures above 20°C, with the RF model showing the highest accuracy in detecting temperatures above and below 20°C based on TPR and TNR comparisons (Table 4).

Based on the statistical metrics, it can be concluded that all models exhibit good accuracy, but the RF and SVM models outperform the other three models overall.

Table4- Comparison different machine learning model's accuracy

Model	TPR	TNR	TSS	MAE	MSE	RMSE	R-squared
ANN	0.74	0.84	0.58	1.62	4.54	1.27	0.55

CART	0.73	0.82	0.55	1.68	4.76	1.30	0.50
SVM	0.82	0.85	0.67	1.28	3.13	1.13	0.68
GLM	0.72	0.82	0.54	1.77	5.40	1.33	0.44
RF	0.82	0.90	0.73	1.11	2.33	1.06	0.76

4.7. Analysis of VIP

A VIP analysis was conducted to evaluate and compare the influence of various parameters on LST. The results indicate that the importance of each parameter varies across different models. On average, the weighted importance of the parameters NDVI, BH, SVF, MPI, and BD was higher than other parameters in the ANN model. In contrast, the top five crucial parameters for the CART and RF models were NDVI, BH, SVF, MPI, and RL. The SVM model identified NDVI, BH, SVF, RA, and Integ_Rn as the most essential parameters, while in the GLM model, NDVI, BH, SVF, RA, and BD were deemed the most significant. Overall, urban morphology parameters (BH, BD, and SVF), vegetation cover parameters (NDVI and MPI) were identified as the most influential factors affecting LST in Tehran (Table 5).

Table 5 - Analysis the importance of various explanatory factors or predictors in the used machine learning models

Parameter	ANN	CART	SVM	GLM	RF
NDVI	1.308	1.306	1.189	1.353	1.168
BH	1.282	1.304	1.156	1.350	1.081
BD	1.255	1.288	1.131	1.338	1.057
SVF	1.272	1.300	1.152	1.336	1.074
RL	1.252	1.297	1.143	1.341	1.064
RA	1.248	1.286	1.150	1.340	1.064
Integ_Rn	1.251	1.287	1.144	1.333	1.064
MPI	1.266	1.292	1.140	1.338	1.065
MPFD	1.247	1.292	1.143	1.328	1.064

4.8. Analysis of LST Using Ensemble Models

The results of LST analysis using ensemble models were presented as maps (Figure 8). The findings show that the Genius King and U.S. Congress methods were more successful in detecting temperatures above 25°C. These two methods estimated that approximately 1% of the study area had temperatures exceeding 25°C, closer to the observed value of 6% obtained through remote sensing compared to the other ensemble models.

Statistical analysis revealed that the influence of each model's vote varies across different ensemble models. Generally, the most effective method maximizes the use of more accurate models. Talent identification enables the selection of the most accurate method, allowing greater reliance on the votes of stronger models. Statistical comparisons showed that the Mean, Weighted Mean, and U.S. Presidential Election methods utilized all models equally. However, the Weighted Mean and U.S. Presidential Election methods incorporated talent identification, whereas the Mean method did not account for the ability or talent of each model. In the Median method, the SVM model had the most significant influence on the final result (24%), followed by the ANN model (22%), while the GLM model contributed to only 13% of the decisions. In the Genius King method, the RF model contributed to 95% of the decisions, followed by the SVM model (37%), while the ANN model, with a 32% frequency, participated only in general votes. In the Ancient Senate method, all models had nearly equal

influence (approximately 20% each) on the final result, as this method does not rely on talent identification but rather on the majority vote. In the U.S. Congress method, only 32% of decisions were made through general voting. Talent identification was precisely implemented, with 68% of decisions made by specialized committees comprising at least three models. Among these, RF and SVM had the highest influence on committee decisions, with frequencies of 22% and 21%, respectively, while GLM participated in only 4% of committee decisions. Additionally, ANN and CART contributed to 13% and 7% of the specialized committee decisions, respectively (Table 6).

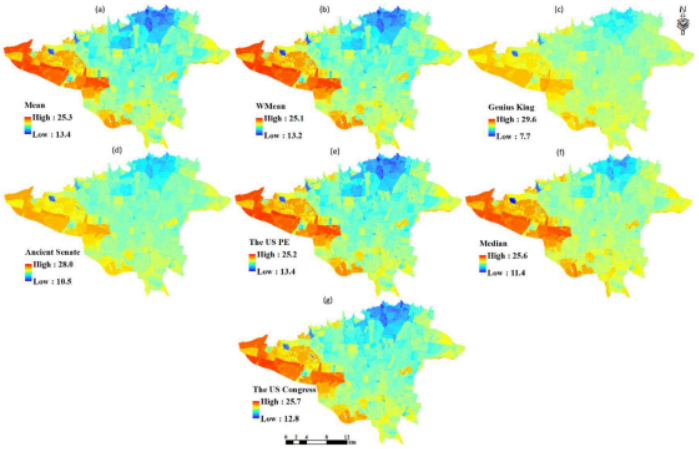

Fig. 8- Predicted LST using Ensemble Modeling

Table 6: Influence of Each Model in Different Ensemble Models (%)

Ensemble Modeling	ANN	CART	SVM	GLM	RF	General Election
Mean	100	100	100	100	100	100
WMean	100	100	100	100	100	100
Median	22	21	24	13	21	0
Genoius_King	32	33	37	33	95	32
Ancient Senate	20.3	19.9	20.4	19.7	19.7	0
The US P.E	100	100	100	100	100	100
The U.S. Congress	45	39	54	37	55	32

4.9. Validation Assessment of Ensemble Models

Validation was conducted using the statistical metrics MAE, MSE, RMSE, and R-squared (R^2) to evaluate the accuracy of the ensemble models and compare them with each other. The MAE values for the Genius King, Weighted Mean (WMean), Median, U.S. Congress, U.S. Presidential Election, Ancient Senate, and Mean methods were 1.31, 1.38, 1.38, 1.39, 1.41, 1.41, and 1.41, respectively. The MSE values for these methods were 3.03, 3.27, 3.33, 3.33, 3.39, 3.42, and 3.43, respectively. The RMSE values were also 1.14, 1.17, 1.18, 1.18, 1.19, 1.19, and 1.19 for the Genius King, WMean, Median, U.S. Congress, U.S. Presidential Election, Ancient Senate, and Mean methods, respectively. Overall, the

Genius King method demonstrated higher accuracy compared to the other ensemble models in analysing LST in the Tehran metropolitan area (Table 7).

A comparison of the TPR and TNR parameters of the ensemble models (Table 7) with those of the individual models (Table 4) indicates that the ensemble models performed better in detecting areas with temperatures above 20°C. Specifically, the TPR for ensemble models ranged from 0.88 to 0.98, while the TPR for individual models ranged from 0.72 to 0.82. Similarly, the TNR for ensemble models ranged from 0.97 to 1.00, compared to a range of 0.82 to 0.92 for the individual models. Furthermore, the MAE, MSE, RMSE, and R^2 metrics demonstrate that ensemble models enhance confidence in the results and improve prediction accuracy.

Table7- Comparison different Ensemble Modeling's accuracy

Ensembling	TPR	TNR	TSS	MAE	MSE	RMSE	R-squared
Mean	0.89	0.98	0.87	1.41	3.42	1.19	0.65
Wmean	0.90	0.98	0.88	1.38	3.27	1.17	0.67
Median	0.90	0.97	0.87	1.38	3.33	1.18	0.66
Genius King	0.98	1.00	0.98	1.31	3.03	1.14	0.69
Ancient Senate	0.91	0.98	0.88	1.41	3.43	1.19	0.65
The US P.E	0.88	0.98	0.86	1.41	3.39	1.19	0.65
The US Congress	0.91	0.98	0.88	1.39	3.33	1.18	0.66

4.10. Analysis of VIP Using Ensemble Models

To evaluate and compare the influence of various parameters on LST using ensemble models, a Variable Importance in Prediction (VIP) analysis was conducted. The results revealed that the importance of each parameter varies across different ensemble models. Despite these differences, the parameters NDVI, BH, MPI, RL, and Integ_Rn consistently exhibited greater importance in the ensemble models than other parameters (Table 8).

Table8- Analysis the importance of various explanatory factors or predictors in the Ensemble Modeling

Model	Mean	WMean	Median	Genoius_King	Ancient Senate	The_US_P.E	The_U.S._Congress
NDVI	1.234	1.222	1.226	1.205	1.229	1.232	1.229
BH	1.201	1.184	1.188	1.152	1.198	1.197	1.189
BD	1.188	1.170	1.180	1.119	1.186	1.184	1.175
SVF	1.190	1.173	1.176	1.131	1.189	1.187	1.178
RL	1.194	1.179	1.176	1.147	1.192	1.191	1.184
RA	1.185	1.167	1.167	1.108	1.184	1.181	1.171
Integ_Rn	1.194	1.179	1.181	1.147	1.191	1.191	1.184
MPI	1.198	1.182	1.187	1.149	1.197	1.195	1.186
MPFD	1.186	1.170	1.175	1.125	1.185	1.183	1.175

5. Discussion

The application of machine learning in addressing complex issues, such as land surface temperature (LST) variations, can significantly enhance the precision and reliability of planning efforts. Ensemble models reduce errors and increase confidence in the results by simultaneously leveraging multiple algorithms. A key aspect of studying LST is identifying and prioritizing factors exacerbating

temperature increases. Given the distinct approaches of different algorithms in analyzing this issue, employing multiple algorithms, assessing their accuracy, and comparing their performance can improve our ability to select the most accurate model, thereby enabling more precise analysis of environmental challenges. For instance, Tanuri et al. demonstrated the remarkable capability of Deep Neural Networks (DNNs) and Extreme Gradient Boosting (XGB) in analyzing LST in Shiraz, while Gourav Suthar et al. (2024) identified ANNs as the most accurate model for predicting LST using air pollution and urban parameter data. Today, various machine learning models are widely used to address environmental issues.

In this study, machine learning was employed to investigate LST variations as an environmental hazard in Tehran, the capital of Iran. Five machine learning models, ANN, RF, SVM, CART, and GLM, were applied to analyse LST. The results indicate varying levels of accuracy among the models in predicting environmental phenomena and hazards. Although all five models demonstrated sufficient accuracy, the RF and SVM models outperformed the other three, while the GLM model exhibited the lowest accuracy. The RF model's superiority aligns with Fei Feng's findings (2024). Conversely, Chaitanya Baliram Pande et al. (2024) highlighted the superior performance of the Bagging ensemble model over XG-Boost and AdaBoost.

Due to the differing computational approaches of the models, the extent of areas with temperatures exceeding 25°C varied across models. The ANN, RF, SVM, and GLM models identified larger areas with temperatures above 25°C, whereas the CART model failed to detect such regions. The results also revealed that all parameters used in this study influenced LST, but their importance varied across models due to differences in how each model estimates relationships between parameters. Despite these variations, urban morphology and green space parameters generally exhibited greater importance than other factors. The influence of urban morphology on LST was also noted in Tanuri et al. (2024). Consequently, future strategies to mitigate rising urban temperatures could focus on reducing BH and density while increasing urban green spaces. Addressing environmental challenges like rising LST requires long-term planning and reversing unsustainable urban development and industrial practices.

The introduction of novel ensemble models and the evaluation of their accuracy in addressing the environmental issue of rising LST demonstrated their effectiveness in enhancing precision and reliability. As these methods are inspired by human collectives, such as the U.S. Congress, presidential elections, monarchical governance, and ancient Senate systems, the results obtained from ensemble models are more reliable than those from a single model. This study's findings confirm that ensemble models can reduce errors and increase confidence by incorporating the strengths of each model. The more adept these methods are at identifying model talents, the lower the error in the resulting predictions. The analysis revealed that the accuracy of ensemble models varied, with the Genius King and Weighted Mean methods demonstrating higher accuracy than others, while the Ancient Senate method exhibited the lowest accuracy and highest error. The Genius King method excelled in talent identification, whereas the Ancient Senate method relied solely on majority voting without considering model capabilities. These findings align with previous studies, such as Ashrafzadeh et al. (2023), which showed that ensemble models generally outperform most individual algorithms in accuracy and precision. Similarly, Achu et al. (2023) demonstrated that ensemble models (Mean, Weighted Mean, Median, and Committee Averaging) increase optimism, yield more accurate results, and reduce uncertainty compared to individual models.

Ensemble models can also be leveraged to analyze parameter importance. The VIP analysis using ensemble models confirmed that NDVI, BH, MPI, RL, and Integ_Rn were the most influential parameters, validating the results of individual algorithms. However, ensemble models provided greater confidence in these findings by considering the outputs of all models. These methods reaffirmed the significant role of urban morphology and green spaces in influencing LST, reinforcing the conclusion that proper urban design is a key strategy for controlling LST in urban areas.

6. Conclusion

Given the fundamental differences in how each algorithm approaches and solves problems, ensemble models offer a valuable solution for consolidating results from multiple models. Moreover, introducing novel ensemble models enhances confidence in the outcomes derived from various algorithms. The ensemble models proposed in this study are inspired by human decision-making processes, where consultation and collaboration lead to successful outcomes. Validation of an issue by multiple models naturally instills greater audience confidence than validation by a single model. Ensemble models the optimal approach for synthesizing the results of multiple models and delivering an outcome. The findings of this study confirm the positive impact of novel ensemble models in improving prediction accuracy and increasing confidence in the results. This issue is particularly significant as the proposed methods are derived from human collectives, and the decisions made closely resemble human group decision-making processes. However, the results are directly influenced by the extent and method of talent identification. In cases where talent identification was more effective and the influence of more accurate models was emphasized, the ensemble results exhibited lower error and higher accuracy. Conversely, in cases where decisions were based solely on majority voting without considering model capabilities, the results deviated more from reality, leading to increased error.

References

1. Aliakbari Bidokhti, A., Hamidianpour, M., & Keshavarz, M. (2016). Trend analysis of temperature and precipitation in Tehran during the period of 1961–2010. *Atmospheric Research, 176-177*, 13-22.
2. Kovats, R. S., & Hajat, S. (2008). Heat stress and public health: a review. *Annual Review of Public Health, 29*, 41-55.
3. Li, X., Zhou, Y., Zhao, M., & Zhao, W. (2017). A meta-analysis of remote sensing-based studies on the relationship between land surface temperature and land use/land cover. *Remote Sensing, 9*(12), 1320.
4. Oke, T. R. (1982). The energetic basis of the urban heat island. *Quarterly Journal of the Royal Meteorological Society, 108*(455), 1-24.
5. Santamouris, M. (2001). Energy and climate in the urban built environment. James & James Science Publishers.
6. Weng, Q., Liu, H., & Lu, D. (2004). Assessing the impact of land use and land cover change on urban surface temperature. *Remote Sensing of Environment, 89*(4), 467-483.
7. Zhang, X., Friedl, M. A., Anderson, M. C., Johnson, D. M., Redmond, K., & Morisette, J. T. (2017). MODIS-based land surface temperature dynamics and relations to

vegetation indices across the conterminous United States. *Remote Sensing of Environment, 189*, 133-148.

8. Aliakbari Bidokhti, A., Hamidianpour, M., & Keshavarz, M. (2016). Trend analysis of temperature and precipitation in Tehran during the period of 1961–2010. *Atmospheric Research, 176-177*, 13-22.
9. Aliakbari Bidokhti, A., Hamidianpour, M., & Keshavarz, M. (2016). Trend analysis of temperature and precipitation in Tehran during the period of 1961–2010. Atmospheric Research, 176-177, 13-22.
10. Gartland, L. (2008). Heat islands: Understanding and mitigating heat in urban areas. Earths can.
11. Kovats, R. S., & Hajat, S. (2008). Heat stress and public health: a review. Annual Review of Public Health, 29, 41-55.
12. Li, X., Zhou, Y., Zhao, M., & Zhao, W. (2017). A meta-analysis of remote sensing-based studies on the relationship between land surface temperature and land use/land cover. Remote Sensing, 9(12), 1320.
13. Oke, T. R. (1982). The energetic basis of the urban heat island. Quarterly Journal of the Royal Meteorological Society, 108(455), 1-24.
14. Santamouris, M. (2001). Energy and climate in the urban built environment. James & James Science Publishers.
15. Taha, H. (1996). Modeling urban albedo impacts on daytime temperature in the urban environment. Atmospheric Environment, 31(17), 2803-2818.
16. Voogt, J. A., & Oke, T. R. (2003). Thermal remote sensing of urban climates. Remote Sensing of Environment, 86(3), 370-384.
17. Weng, Q., Liu, H., & Lu, D. (2004). Assessing the impact of land use and land cover change on urban surface temperature. Remote Sensing of Environment, 89(4), 467-483.
18. Zhang, X., Friedl, M. A., Anderson, M. C., Johnson, D. M., Redmond, K., & Morisette, J. T. (2017). MODIS-based land surface temperature dynamics and relations to vegetation indices across the conterminous United States. Remote Sensing of Environment, 189, 133-148.
19. Statistical Center of Iran(2021), Results of the General Population and Housing Census 2016.

20. Ashrafzadeh, M. R., Shahbazinasab, K., Mohammadi, A., & Penteriani, V. (2023). Determining the distribution factors of an endangered large carnivore: A case study of the brown bear Ursus arctos population in the Central Zagros Mountains, Southwest Iran. *Global Ecology and Conservation*, *46*, e02590.
21. L., Achu & C D, Aju & Di Napoli, Mariano & Prakash, Pranav & Gopinath, Girish & E., Shaji & Chandra S S, Vinod. (2023). Machine-learning based landslide susceptibility modelling with emphasis on uncertainty analysis. Geoscience Frontiers. 101657. 10.1016/j.gsf.2023.101657 .
22. Fleming, S.W., Watson, J.R., Ellenson, A., Cannon, A.J., Vesselinov, V.C., 2021. Machine learning in earth and environmental science requires education and research policy reforms. Nat. Geosci. 14, 878–880. https://doi.org/10.1038/s41561-021-00865-3.
23. G evaert, C.M., 2022. Explainable AI for earth observation: a review including societal and regulatory perspectives. Int. J. Appl. Earth Obs. Geoinf. 112, 102869 https://doi.org/10.1016/j.jag.2022.102869.
24. G unning, D., Stefik, M., Choi, J., Miller, T., Stumpf, S., Yang, G.-Z., 2019. XAI-Explainable artificial intelligence. Sci. Robot. 4 https://doi.org/10.1126/scirobotics. aay7120 eaay7120.
25. McGovern, A., Lagerquist, R., John Gagne, D., Jergensen, G.E., Elmore, K.L., Homeyer, C.R., Smith, T., 2019. Making the black box more transparent: understanding the physical implications of machine learning. Bull. Am. Meteorol. Soc. 2175–2199. https://doi.org/10.1175/BAMS-D-18-0195.1.
26. Gholamreza Roshan, Saleh Arekhi, Zainab Bayganeh, Shady Attia, Evaluation of the intensity of urban heat islands during heat waves using local climate zones in the semi-arid, continental climate of Tehran, Urban Climate, Volume 56, 2024, 102079, ISSN 2212-0955, https://doi.org/10.1016/j.uclim.2024.102079.(https://www.sciencedirect.com/science/article/pii/S221209552400275X)
27. Majid Kiavarz, Sara Bourbour Hosseinbeigi, Naeim Mijani, Mohammad Sina Shahsavary, Mohammad Karimi Firozjaei, Predicting spatial and temporal changes in surface urban heat islands using multi-temporal satellite imagery: A case study of Tehran metropolis,Urban Climate,Volume 45,2022,101258,ISSN22120955,https://doi.org/10.1016/j.uclim.2022.101258.(https://www.sciencedirect.com/science/article/ii/S2212095522001766)
28. Ghazaleh Tanoori, Ali Soltani, Atoosa Modiri, Machine Learning for Urban Heat Island (UHI) Analysis: Predicting Land Surface Temperature (LST)in Urban Environments,Urban Climate,Volume

55,2024,101962,ISSN22120955,https://doi.org/10.1016/j.uclim.2024.101962.(https://www.sciencedirect.com/science/article/pii/S2212095524001585)

29. Fei Feng, Yaxue Ren, Chengyang Xu, Baoquan Jia, Shengbiao Wu, Raffaele Lafortezza,Exploring the non-linear impacts of urban features on land surface temperature using explainable artificial intelligence,Urban Climate,Volume 56,2024,102045,ISSN 22120955,https://doi.org/10.1016/j.uclim.2024.102045.(https://www.sciencedirect.com/science/article/pii/2212095524002414)
30. Gourav Suthar, Nivedita Kaul, Sumit Khandelwal, Saurabh Singh,Predicting land surface temperature and examining its relationship with air pollution and urban parameters in Bengaluru: A machine learning approach,Urban Climate,Volume 53,2024,101830,ISSN 2212-0955,https://doi.org/10.1016/j.uclim.2024.101830.(https://www.sciencedirect.com/science/article/pii/S2212095524000269)
31. Irshad, Z., Hassan, M., Akbar, S., Farooq, M., & Chishtie, F. A. (2024). Spatiotemporal changes in LULC and associated impact on urban Heat Islands over Pakistan using geospatial techniques. *Urban Climate*, *57*, 102112.
32. Chaitanya Baliram Pande, Johnbosco C. Egbueri, Romulus Costache, Lariyah Mohd Sidek, Qingzheng Wang, Fahad Alshehri, Norashidah Md Din, Vinay Kumar Gautam, Subodh Chandra Pal,Predictive modeling of land surface temperature (LST) based on Landsat-8 satellite data and machine learning models for sustainable development,Journal of Cleaner Production,Volume 444,2024,141035,ISSN 0959-6526,https://doi.org/10.1016/j.jclepro.2024.141035.
33. Liu, X., Huang, Y., Xu, X., et al., 2020. High-spatiotemporal-resolution mapping of global urban change from 1985 to 2015. Nat Sustain 3, 564–570. https://doi.org/ 10.1038/s41893-020-0521-x.
34. Li, C., Song, Y., Kaza, N., Burghardt, R., 2023. Explaining spatial variations in residential energy usage intensity in Chicago: the role of urban form and Geomorphometry. J. Plan. Educ. Res. 43 (2), 317–331. https://doi.org/10.1177/0739456X19873382.
35. Halder, B., Bandyopadhyay, J., Banik, P., 2021. Monitoring the effect of urban development on urban heat island based on remote sensing and geo-spatial approach in Kolkata and adjacent areas, India. Sustain. Cities Soc. 74, 103186. ISSN 2210-6707. https://doi.org/10.1016/j.scs.2021.103186.
36. Jiang, Y., Lin, W.P., Xu, D., Xu, D., 2023. Spatio-temporal variation of the relationship between air pollutants and land surface temperature in the Yangtze River Delta urban agglomeration China. Sustain Cities Soc. 91, 104429. https://doi.org/10.1016/j.scs.2023.104429.

37. Z hang, N., Zhang, J., Chen, W., Su, J., 2022. Block-based variations in the impact of characteristics of urban functional zones on the urban heat island effect: a case study of Beijing. Sustain. Cities Soc. 76, 2210–6727. https://doi.org/10.1016/j.scs.2021.103529.
38. Buyantuyev, A., Wu, J., 2009. Urban heat islands and landscape heterogeneity: linking spatiotemporal variations in surface temperatures to land-cover andsocioeconomic patterns. Landsc. Ecol. 25 (1), 17–33. https://doi.org/10.1007/s10980-009-9402-4.
39. Connors, J.P., Galletti, C.S., Chow, W.T.L., 2013. Landscape configuration and urban heat island effects: assessing the relationship between landscape characteristics and land surface temperature in Phoenix Arizona. Landsc. Ecol. 28 (2), 271–283. https://doi.org/10.1007/s10980-012-9833-1.
40. Ren, Z., Wang, C., Guo, Y., et al., 2024. The cooling capacity of urban vegetation and its driving force under extreme hot weather: a comparative study between dry- hot and humid-hot cities[J]. Build. Environ. 263, 111901. https://doi.org/10.1016/j.buildenv.2024.111901.
41. Takebayashi, H., Moriyama, M., 2007. Surface heat budget on green roof and high reflection roof for mitigation of urban heat island. Build. Environ. 42 (8), 2971–2979. https://doi.org/10.1016/j.buildenv.2006.06.017.
42. Takebayashi, H., Moriyama, M., 2012. Study on surface heat budget of various pavements for urban heat island mitigation. Adv. Mater. Sci. Eng. 523051, 11 Pages. https://doi.org/10.1155/2012/523051.
43. Oke, T.R., Mills, G., Christen, A., Voogt, J.A., 2017. Urban climates. Cambridge university press.Oliveira, A.M., Kjerfve, B., 1993. Environmental responses of a tropical coastal lagoon system tohydrological variability: Mundau-manguaba, Brazil. Estuar. Coast.Shelf Sci. 37, 575–591.
44. Magli, S., Lodi, C., Lombroso, L., Muscio, A., Teggi, S., 2015. Analysis of the urban heat island effects on building energy consumption. Int. J. Energy Environ. Eng. 6, 91–99.
45. U. Nations, World urbanization prospects, https://population.un.org/wup/Publications/Files/WUP2018 Report.pdf, 2018.Uddin, A.S., Khan, N., Islam, A.R.M.T., Kamruzzaman, M., Shahid, S., 2022. Changes in urbanization and urban heat island effect in Dhaka City. Theor. Appl. Climatol.147, 891–907.
46. Vinayak, B., Lee, H.S., Gedam, S., Latha, R., 2022. Impacts of future urbanization on urban microclimate and thermal comfort over the Mumbai metropolitan region,India. Sustain. Cities Soc. 79, 103703.
47. de Souza, D.O., dos Santos Alval´a, R.C., do Nascimento, M.G., 2016. Urbanization effects on the microclimate of Manaus: a modeling study. Atmos. Res. 167, 237–248.dos Santos, E.C.,

Sampaio, C.L.S., 2013. A pesca artesanal na comunidade de fern˜ao velho, maceí´o (alagoas, brasil): de tradicional a marginal. Revista de Gest˜ao Costeira Integrada-Journal of Integrated Coastal Zone Management 13, 513–524.

48. Morris, K.I., Chan, A., Morris, K.J.K., Ooi, M.C., Oozeer, M.Y., Abakr, Y.A., Nadzir, M.S.M., Mohammed, I.Y., Al-Qrimli, H.F., 2017. Impact of urbanization level on theinteractions of urban area, the urban climate, and human thermal comfort. Appl. Geogr. 79, 50–72.
49. Dadashpoor, H., Azizi, P., Moghadasi, M., 2019. Land use change, urbanization, and change in landscape pattern in a metropolitan area. Sci. Total Environ. 655,707–719.
50. Lin, P., Lau, S.S.Y., Qin, H., Gou, Z., 2017. Effects of urban planning indicators on urban heat island: a case study of pocket parks in high-rise high-density environment. Landsc. Urban Plan. 168, 48–60.
51. Zhou, M., Wang, R., Guo, Y., 2024. How urban spatial characteristics impact surface urban heat island in subtropical high-density cities based on LCZs: a case study of Macau. Sustain. Cities Soc. 112, 105587.

ZandiPaper.docx

ORIGINALITY REPORT

18%
SIMILARITY INDEX

PRIMARY SOURCES

1	www.ncbi.nlm.nih.gov Internet	259 words —	4%
2	Rahman Zandi, Ghasem Shah Pari Far. "Evaluating the factors affecting landslides using machine learning algorithms (case study: the catchment area of Karun-3 Dam, Iran)", The Egyptian Journal of Remote Sensing and Space Sciences, 2025 Crossref	208 words —	3%
3	www.mdpi.com Internet	96 words —	1%
4	www.rbz.co.zw Internet	58 words —	1%
5	moam.info Internet	40 words —	1%
6	www.frontiersin.org Internet	38 words —	1%
7	link.springer.com Internet	27 words —	< 1%
8	Hala M. Alshamlan. "DQB: A novel dynamic quantitive classification model using artificial bee	21 words —	< 1%

colony algorithm with application on gene expression profiles", Saudi Journal of Biological Sciences, 2018
Crossref

9 www.ijirset.com
Internet
21 words — < 1%

10 assets-eu.researchsquare.com
Internet
20 words — < 1%

11 Hardy, Caroline Hazel. "Analyzing the Urban Heat Island Effect Using Remotely Sensed Data.", University of Johannesburg (South Africa), 2024
ProQuest
19 words — < 1%

12 Soumik Saha, Sumana Bhattacharjee, Pravat Kumar Shit, Nairita Sengupta, Biswajit Bera. "Deforestation probability assessment using integrated machine learning algorithms of Eastern Himalayan foothills (India)", Resources, Conservation & Recycling Advances, 2022
Crossref
19 words — < 1%

13 ijettjournal.org
Internet
18 words — < 1%

14 Wang, Jifei. "Investigating the Effects of 2D and 3D Urban Morphology on the Land Surface Temperature Using GIS and Remote Sensing", National University of Singapore (Singapore), 2025
ProQuest
17 words — < 1%

15 Iacopo Carnacina, Mawada Abdellatif, Manolia Andredaki, James Cooper, Darren Lumbroso, Virginia Ruiz-Villanueva. "River Flow 2024", CRC Press, 2025
Publications
16 words — < 1%

16 Ghazaleh Tanoori, Ali Soltani, Atoosa Modiri. "Machine Learning for Urban Heat Island (UHI)
15 words — < 1%

Analysis: Predicting Land Surface Temperature (LST) in Urban Environments", Urban Climate, 2024
Crossref

17 Shitian Luo, Peng Ren. "A thermal diffusion-guided method for filling gaps in urban ECOSTRESS land surface temperature during summer", Building and Environment, 2026 — 14 words — < 1%
Crossref

18 ricerca.uniba.it — 14 words — < 1%
Internet

19 Naeim Mijani, Seyed Kazem Alavipanah, Saeid Hamzeh, Mohammad Karimi Firozjaei, Jamal Jokar Arsanjani. "Modeling thermal comfort in different condition of mind using satellite images: An Ordered Weighted Averaging approach and a case study", Ecological Indicators, 2019 — 13 words — < 1%
Crossref

20 Shuo Zhang, Xiaoyi Fang, Chen Cheng, Liuxin Chen, Li Zhang, Ying Yu, Lei Li, Hongyan Luo. "Research on the Planning Method and Strategy of Urban Wind and Heat Environment Optimization—Taking Shenzhen, a Sub-Tropical Megacity in Southern China, as an Example", Atmosphere, 2022 — 13 words — < 1%
Crossref

21 "Biomonitoring of Pollutants in the Global South", Springer Science and Business Media LLC, 2024 — 11 words — < 1%
Crossref

22 Patrick Samson Udama Eneche, Funda Atun, Yijian Zeng, Karin Pfeffer. "Robust drivers of urban land surface temperature dynamics across diverse — 11 words — < 1%

landscape characters: An augmented systematic literature review", Ecological Indicators, 2024
Crossref

23 Rahim Maleknia. "Roots of urban forest conservation behaviors: Discovering determinants of citizens' attitudes", Environmental and Sustainability Indicators, 2025 — 11 words — < 1%
Crossref

24 repositorio.uloyola.es — 11 words — < 1%
Internet

25 public-pages-files-2025.frontiersin.org — 10 words — < 1%
Internet

26 www.researchgate.net — 10 words — < 1%
Internet

27 Agnieszka Sutkowska, Andrzej Pasierbiński, Tomasz Warzecha, Abul Mandal, Józef Mitka. "REFUGIAL PATTERN OF BROMUS ERECTUS IN CENTRAL EUROPE BASED ON ISSR FINGERPRINTING", Acta Biologica Cracoviensia Series Botanica, 2013 — 9 words — < 1%
Crossref

28 King, Parker. "Modeling to Evaluate the Contribution of the Built Environment on Heat Microenvironments and Analysis of the Efficiency and Efficacy of Electric Vehicle Purchase Incentives", The University of Vermont and State Agricultural College, 2024 — 9 words — < 1%
ProQuest

29 Xitian Cai, Luyi Li, Joshua B. Fisher, Zhenzhong Zeng, Sha Zhou, Xuezhi Tan, Bingjun Liu, Xiaohong Chen. "The responses of ecosystem water use efficiency to — 9 words — < 1%

CO2, nitrogen deposition, and climatic drivers across China", Journal of Hydrology, 2023
Crossref

30	amazoniainvestiga.info Internet	9 words — < 1%
31	d-nb.info Internet	9 words — < 1%
32	eprints.qut.edu.au Internet	9 words — < 1%
33	espace.curtin.edu.au Internet	9 words — < 1%
34	Chaitanya Baliram Pande, Johnbosco C. Egbueri, Romulus Costache, Lariyah Mohd Sidek et al. "Predictive modeling of land surface temperature (LST) based on Landsat-8 satellite data and machine learning models for sustainable development", Journal of Cleaner Production, 2024 Crossref	8 words — < 1%
35	Gourav Suthar, Saurabh Singh, Nivedita Kaul, Sumit Khandelwal. "Exploring urban heat dynamics through multi-model machine learning analysis of land surface temperature in Bengaluru India", Natural Hazards, 2025 Crossref	8 words — < 1%
36	Hadi Soltanifard, Abdolreza Kashki, Mokhtar Karami. "Analysis of spatially varying relationships between urban environment factors and land surface temperature in Mashhad city, Iran", The Egyptian Journal of Remote Sensing and Space Science, 2022 Crossref	8 words — < 1%

37 Hamid Jahankhani, Gordon Bowen, Nitsa J. Herzog, David J. Herzog. "Symbiotic Intelligence - Advancing Forecasting Through Human-AI Collaboration", CRC Press, 2025 — 8 words — < 1%
Publications

38 Jaekyoung Kim, Samuel Park, Seungkwon Jung, Gunwon Lee. "Urban cold stress assessment using computational fluid dynamics and universal thermal climate index: A case study of Gwacheon City, South Korea", Sustainable Cities and Society, 2025 — 8 words — < 1%
Crossref

39 Khurshid, Hamna. "Rawalpindi's Urban Heat Island: Exploring Landscape Dynamics and Thermal Patterns", Universidade NOVA de Lisboa (Portugal) — 8 words — < 1%
ProQuest

40 Lee, So Young. "Spatial Dynamics of Residential Neighborhoods and Urban Amenities", National University of Singapore (Singapore), 2025 — 8 words — < 1%
ProQuest

41 Matheus Schmidt, Samuel Nelson Melegari de Souza, Deonir Secco, Aline Snak, Doglas Bassegio. "Evaluation of thermal performance in green roofs using recycled construction waste sand as substrate", Urban Ecosystems, 2024 — 8 words — < 1%
Crossref

42 S.P. Jani, M. Adam Khan. "Applications of AI in Smart Technologies and Manufacturing", CRC Press, 2025 — 8 words — < 1%
Publications

43 Sang-Hyun Lee. "Further Development of the Vegetated Urban Canopy Model Including a Grass- — 8 words — < 1%

Covered Surface Parametrization and Photosynthesis Effects", Boundary-Layer Meteorology, 2011
Crossref

44 Taghavi, Nasrin. "Developing a Geospatial Bayesian Probabilistic Method for Groundwater Vulnerability Assessment", University of New South Wales (Australia)
ProQuest
8 words — < 1%

45 Wenze Li, Wenchao Han, Jiachen Meng, Zipeng Dong, Jun Xu, Qimeng Wang, Lulu Yuan, Han Wang, Zhongzhi Zhang, Miaomiao Cheng. "Machine learning-based generation of high-resolution 3D full-coverage aerosol distribution data over China using multisource data", Remote Sensing of Environment, 2025
Crossref
8 words — < 1%

46 Yuxin Cao, Sheng Liu, Yi Lu, Hongtai Yang, Linchuan Yang. "Multiscale impacts of urban nature on land surface temperature over two decades in a city with cloudy and foggy climates", Urban Climate, 2025
Crossref
8 words — < 1%

47 elib.dlr.de
Internet
8 words — < 1%

48 en.wikipedia.org
Internet
8 words — < 1%

49 journals.blueeyesintelligence.org
Internet
8 words — < 1%

50 library.kpi.kharkov.ua
Internet
8 words — < 1%

51 H.M. Imran, J. Kala, A.W.M. Ng, S. Muthukumaran. "Effectiveness of vegetated patches as Green Infrastructure in mitigating Urban Heat Island effects during a heatwave event in the city of Melbourne", Weather and Climate Extremes, 2019 — 7 words — < 1%
Crossref

52 Parag Verma, Er. Devarasetty Purna Sankar, Anuj Bhardwaj, Vaibhav Chaudhari, Arnav Pandey, Ankur Dumka. "Handbook of Deep Learning Models - Volume One: Fundamentals", CRC Press, 2025 — 7 words — < 1%
Publications

53 "Multi-Scale Model Development for Estimating Urban Air Temperature Patterns Using Land Surface Temperature and Auxiliary Data", University of Szeged, 2025 — 6 words — < 1%
Crossref Posted Content

54 Hamad Ahmed Altuwaijri, Abdulla Al Kafy, Zullyadini A. Rahaman, Md Tanvir Miah et al. "Predicting Spatiotemporal Dynamics of Land Use Influenced Thermal Patterns Using Remote Sensing-based Machine Learning Algorithms", Rangeland Ecology & Management, 2025 — 6 words — < 1%
Crossref

55 R. N. V. Jagan Mohan, B. H. V. S. Rama Krishnam Raju, V. Chandra Sekhar, T. V. K. P. Prasad. "Algorithms in Advanced Artificial Intelligence - Proceedings of International Conference on Algorithms in Advanced Artificial Intelligence (ICAAAI-2024)", CRC Press, 2025 — 6 words — < 1%
Publications

56 Shaofeng Chen, Yuwei Qiu, Yuhan Xu, Jiafang Huang, Zheng Ding. "Modeling and optimization of heat island networks based on machine learning and the — 6 words — < 1%

perspective of spatial heterogeneity in metropolitan areas", Urban Climate, 2025
Crossref

EXCLUDE QUOTES	OFF	EXCLUDE SOURCES	OFF
EXCLUDE BIBLIOGRAPHY	ON	EXCLUDE MATCHES	OFF